AD NUMBER

ADB006808

LIMITATION CHANGES

TO:

Approved for public release; distribution is unlimited.

FROM:

Distribution authorized to U.S. Gov't. agencies only; Test and Evaluation; 25 JUL 1975. Other requests shall be referred to Air Force Cambridge Research Laboratories, Hanscom AFB, MA 01731.

AUTHORITY

AFGL ltr, 7 Sep 1976

AFCRL-TR-75-0403
AIR FORCE SURVEYS IN GEOPHYSICS, NO. 317

Effects of an Irregular Ionosphere on L-Band Radar Systems

SAMUEL HOROWITZ
TERENCE J. ELKINS

25 July 1975

IONOSPHERIC PHYSICS LABORATORY PROJECT 5631
AIR FORCE CAMBRIDGE RESEARCH LABORATORIES
HANSCOM AFB, MASSACHUSETTS 01731

AIR FORCE SYSTEMS COMMAND, USAF

Unclassified

SECURITY CLASSIFICATION OF THIS PAGE (When Data Entered)

REPORT DOCUMENTATION PAGE		READ INSTRUCTIONS BEFORE COMPLETING FORM
1. REPORT NUMBER AFCRL-TR-75-0403	2. GOVT ACCESSION NO.	3. RECIPIENT'S CATALOG NUMBER
4. TITLE (and Subtitle) EFFECTS OF AN IRREGULAR IONOSPHERE ON L-BAND RADAR SYSTEM		5. TYPE OF REPORT & PERIOD COVERED Scientific. Interim. 6. PERFORMING ORG. REPORT NUMBER AFSG No. 317
7. AUTHOR(s) Samuel Horowitz Terence J. Elkins		8. CONTRACT OR GRANT NUMBER(s)
9. PERFORMING ORGANIZATION NAME AND ADDRESS Air Force Cambridge Research Laboratories (LI) Hanscom AFB Massachusetts 01731		10. PROGRAM ELEMENT, PROJECT, TASK AREA & WORK UNIT NUMBERS 61102F 56311601
11. CONTROLLING OFFICE NAME AND ADDRESS Air Force Cambridge Research Laboratories (LI) Hanscom AFB Massachusetts 01731		12. REPORT DATE 25 July 1975 13. NUMBER OF PAGES
14. MONITORING AGENCY NAME & ADDRESS(if different from Controlling Office)		15. SECURITY CLASS. (of this report) Unclassified 15a. DECLASSIFICATION/DOWNGRADING SCHEDULE

16. DISTRIBUTION STATEMENT (of this Report)

Distribution limited to U.S. Government agencies only; (Test and Evaluation); (25 July 1975). Other requests for this document must be referred to AFCRL (LI), Hanscom AFB, Massachusetts 01731.

17. DISTRIBUTION STATEMENT (of the abstract entered in Block 20, if different from Report)

18. SUPPLEMENTARY NOTES

19. KEY WORDS (Continue on reverse side if necessary and identify by block number)

Irregularity reflection
Radar range errors
Ray tracing
Travelling ionospheric disturbance

20. ABSTRACT (Continue on reverse side if necessary and identify by block number)

The change in apparent range between an L-Band Radar System and a high flying target introduced by a travelling ionospheric disturbance (TID) is calculated. Using an ambient Chapman electron density profile perturbated by a realistic TID model, the excess propagation time delay is determined by the use of ray-tracing techniques. For a fixed frequency, the variable component of group delay due to these irregularities is dependent on the direction of TID travel relative to the propagation path and the elevation angle. Numerical results for a typical case are represented.

DD FORM 1 JAN 73 1473 EDITION OF 1 NOV 65 IS OBSOLETE

Unclassified

SECURITY CLASSIFICATION OF THIS PAGE (When Data Entered)

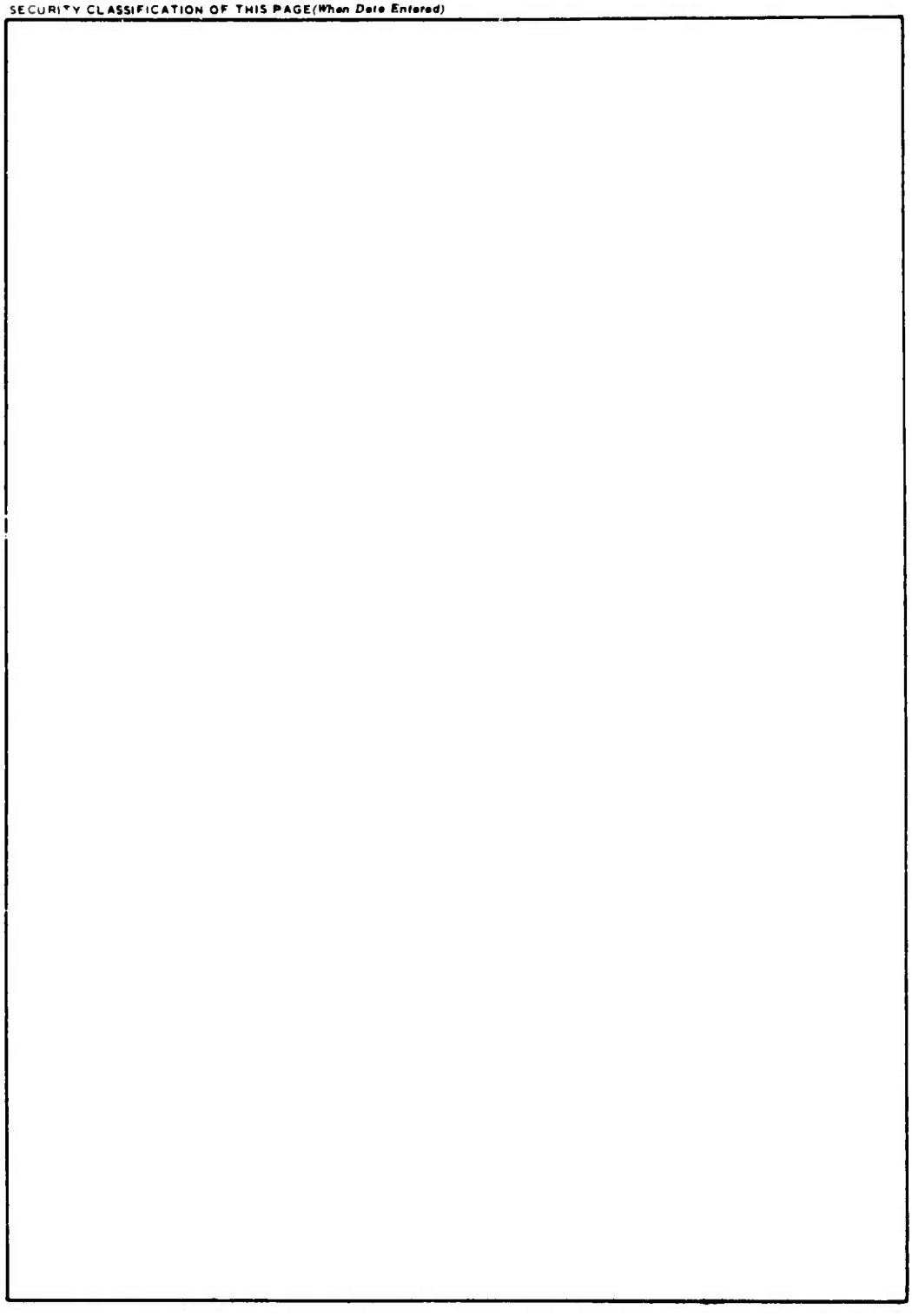

Preface

The authors wish to thank Major John Scheerer and Capt. Richard Durham for the introduction to the problem and helpful discussions.

Contents

Illustrations

Illustrations

Tables

Effects of an Irregular Ionosphere on L-Band Radar Systems

1. INTRODUCTION

L-band radars, such as the Cobra Dane System, employ a multifrequency technique to correct for the range error due to ionospheric retardation of the radar pulse. It is desirable to know over what physical area and time duration this correction factor can be applied and in particular, the influence of TIDs on the Cobra Dane range correction algorithm. This information will assist the system designer in determining the frequency or number of ionospheric measurements required in support of the Cobra Dane Radar to meet a specified ionospheric error budget.

The correction scheme which has been developed to compensate for ionospheric propagation effects in the Cobra Dane Radar assumes that the ionosphere is essentially spherically stratified. It is required here to evaluate the effects on this error correction scheme of non-uniform horizontal ionospheric gradients predominately due to travelling ionospheric disturbances (TIDs) generated by gravity waves. The error manifests itself as refractive bending of the radiowave and retardation which causes the apparent range of the target to be greater than its true range. The intent of this report is to describe the results of a simulation study of the radio wave errors due to propagation in non-uniform irregular ionosphere of an L-band radar pulse. The group delay, apparent range or radar range is calculated by employing

(Received for publication 25 July 1975)

ray-tracing techniques through a model ionosphere where a TID is superimposed on an ambient alpha Chapman electron density profile to simulate a realistic ionosphere.

In Sections 2 and 3 the mechanism and morphology of TIDs are reviewed so that parameters of a realistic gravity wave model of the neutral atmosphere with coupling to the ionized medium can be postulated. Generation of a model ionosphere is described in Section 4. The ray-tracing results are illustrated and discussed in Section 5.

2. MECHANISM OF TIDs

Travelling ionospheric disturbances (TIDs) have been observed by a large number of workers using many different techniques since the pioneering work of Munro.[1] However, it was not until the theoretical work of Hines and Hooke[2,3] that the nature of these disturbances was interpreted successfully as wave-like fluctuations of the electron density induced by gravity waves in the neutral atmosphere. There are two major classes of TIDs, "large scale" and "medium scale".[4] The large scale waves are generally associated with infrequent magnetic storms, whereas the medium scale waves occur much more frequently. Explanation of long-distance propagation by medium-scale TIDs relies on the predominantly horizontal group velocity of freely propagating internal gravity waves, coupled with their tendency to be controlled by the direction of the earth's gravitational field so as to follow the curvature of the earth.[5]

3. MORPHOLOGY OF TID

Elkins[6] has measured the variable component of ionospheric refraction at frequencies in the VHF range. Figure 1 shows the results of a typical day's data,

1. Munro, G. H. (1958) Travelling ionospheric disturbances in the F-region, Aust. J. Phys., 11(1):91-112.
2. Hines, C.O. (1960) Internal atmospheric gravity waves at ionospheric heights, Can. J. Phys., 38(11):1441-1481.
3. Hooke, W. H. (1968) Ionospheric irregularities produced by internal atmospheric gravity waves, J. Atmos. Terr. Phys., 30(5):795-824.
4. Georges, T. M. (1968) HF doppler studies of travelling ionospheric disturbances, J. Atmos. Terr. Phys., 39(5):735-746.
5. Francis, S. H. (1972) Propagation of internal acoustic gravity waves around a spherical earth, J. Geophys. Res., 77:4221.
6. Elkins, T. J. (1972) High resolution measurements of ionospheric refraction, Space Research XII, pp. 1215-1220, Akademie-Verlag, Berlin.

with the magnetic North-South component of refraction angle, in the horizontal plane, plotted as a function of local time, after filtering. Note the pronounced spectral component with a quasi-period ~ 30 to 40 min, with a maximum near local noon. This is a very distinctive feature of all the data obtained. Figure 2 shows the power spectrum of data similar to those of Figure 1, averaged over an interval of 14 successive days. The power per octave is plotted as a function of the period of the fluctuation. There is a pronounced peak of power in the octave centered at 40-min period.

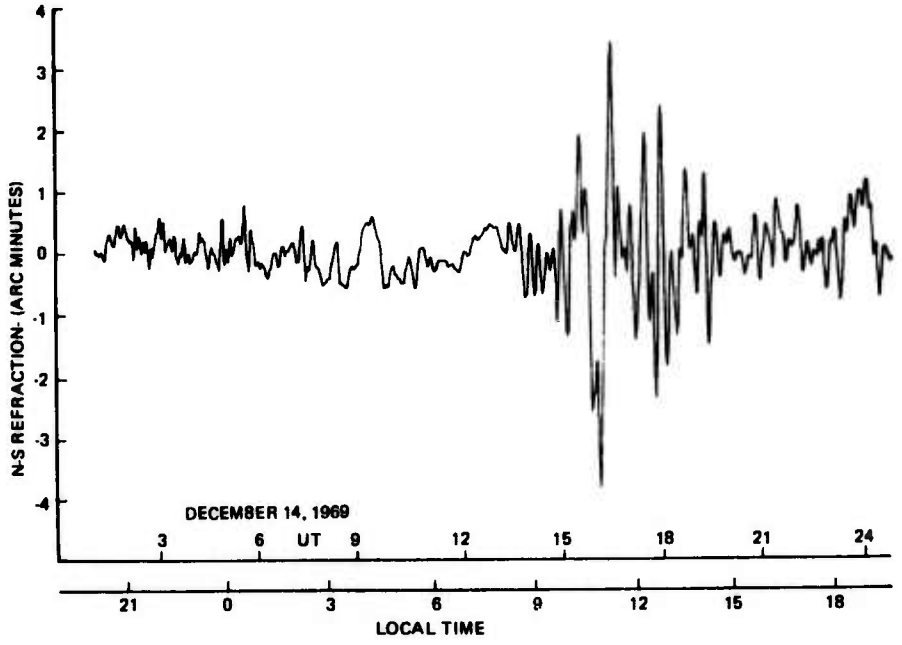

Figure 1. Typical Variation of the North-South Component of Refraction Angle in the Horizontal Plane for One Day, Showing the Diurnal Variation of TID

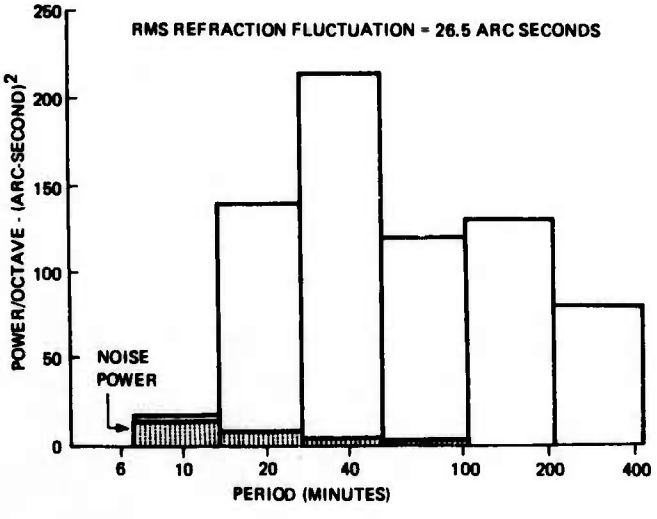

Figure 2. Power Per Octive Contained in the Refraction Fluctuations, as a Function of Period. The figure represents an average over a 14-day interval

Figure 3 shows the monthly average of the rms average from the hourly mean of the fluctuations and, below, the mean fluctuation period, for the periods October 1969 to January 1970 and April to August 1970. From these results several general features are apparent: (1) The diurnal variation is such that the maximum rms fluctuation in refraction occurs within an hour or two of local noon, and (2) the seasonal variation has a weakly defined maximum in November. Note that the periods of recording were such that the coverage near the equinoxes is poor. However, winter values of fluctuation amplitude exceed those for summer; (3) the rms fluctuation, averaged over 24 hrs, is approximately 30 arc sec (at a frequency of 136 MHz), which agrees closely with the estimate obtained from the power spectrum (Figure 2). (At 1215 MHz, the corresponding value would be 0.38 arc sec.)

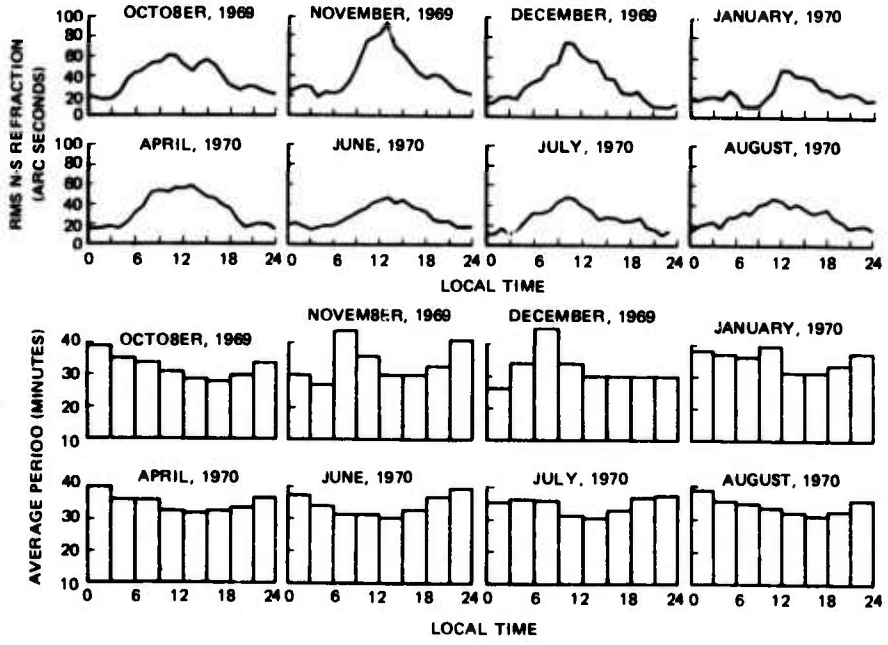

Figure 3. Diurnal Variation of Refraction Fluctuations, for 8 Months' Data: Above, rms Amplitude; Below, Mean Period of Fluctuation

Under the simplifying assumption of horizontal stratification of the ionosphere, the refractive deviation of a ray traversing the entire ionosphere is proportional to the horizontal gradient of the integrated (total) electron content (TEC). A preliminary comparison of refraction measurements with simultaneous TEC data along the identical ray path has shown that this relationship is often approximately satisfied

on a time scale of the order of one hr or less. For longer period fluctuations, this simple approximation appears not to be valid.

The observed refraction fluctuations, caused by TIDs, have been observed by a number of different techniques, over a period of many years. They are currently thought to be a manifestation, in the ionospheric plasma, of internal gravity waves propagating in the neutral thermospheric gas. The sharp decrease of spectral power at the high-frequency end of the spectrum in Figure 2 is consistent with the theoretically predicted evanescent propagation of gravity waves with period shorter than the Brunt period (~ 14 min in the F region). Simultaneous measurement of TEC variations at each end of the interferometer baseline,[6] has consistently indicated a horizontal trace velocity for the waves of ~ 150 m sec^{-1}, which is typical of freely propagating gravity waves with period ~ 35 min.

It has been noted previously, for example, (2) that the amplitude of TIDs appears to be an approximately constant percentage, throughout the day, of the TEC. Thus, greater fluctuation amplitudes are observed during the daytime, when the TEC is high, than at night, when the TEC is low. This effect certainly appears to be responsible for at least part of the diurnal variation of fluctuation amplitude observed. However, closer examination of the data shows that the fluctuation amplitude usually reaches its maximum an hour or two earlier than TEC. This is shown, for the month of November 1969, in Figure 4. The mean refraction amplitude, the mean TEC, and the standard deviation of the TEC variations are shown

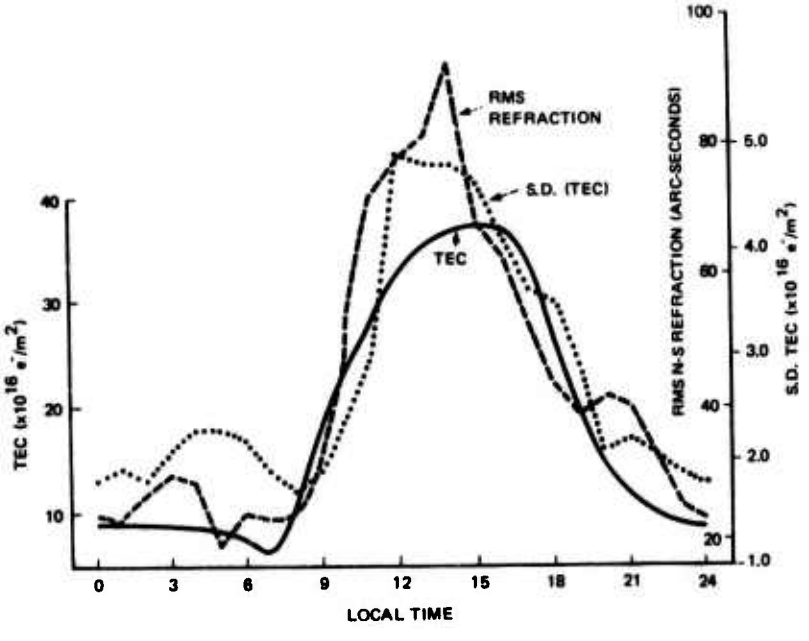

Figure 4. Diurnal Variation of rms Refraction Fluctuation Amplitude, TEC and the Standard Deviation of TEC Variability, for November 1969

as functions of local time. It is highly probable that the TEC variability is predominantly due to TIDs, but the TEC itself reaches its maximum about two hrs later than the fluctuations. This discrepancy may be due to a superposition of a true source effect; that is, the amplitude of the source of the TID may reach maximum shortly before noon, whereas the TEC reaches its maximum at about 1400 local time.

4. IONOSPHERIC MODEL

Before the ray-tracing studies can be performed, a suitable model of the ambient and perturbed ionosphere is required. The ambient ionosphere was chosen to reflect conditions to the North-West of the radar during winter day at sunspot maximum. An alpha Chapman profile was chosen for the vertical electron density distribution, having a scale height of 50 km with a maximum electron density at 250 km. The critical frequency of this layer was chosen to be 12 MHz with a vertical TEC of 3.2×10^{17} electrons/m^2 illustrative of noon condition as shown in Figure 4. The special effects of the auroral ionosphere are not considered.

A moderately strong TID model as described[7] was postulated. The TID was modelled from physical principles by considering the propagation of an internal gravity wave in the neutral gas and computing the induced effects upon the free ionospheric electrons. This model differs from previous models by including dissipation (viscosity and thermal conductivity) and by using a realistic sound speed profile throughout the thermosphere. The model assumes that the wave dependence on the time t and horizontal coordinate x is a sinusoidal function of $t - k_x x$, where k_x is the horizontal wave number. It derives the vertical profile by solving the coupled Navier-Stokes and electron continuity equations. The basic inputs to the model are the wavelength, period, amplitude and azimuth of propagation of the neutral gravity wave underlying the TID which is to be modelled.

The parameters of the model were chosen purposely to reflect moderately strong conditions without being unrealistic. Travelling ionospheric disturbances are always present in the ionosphere - only their amplitude varies in a random manner. The value of 50 m/sec chosen for the amplitude of the neutral gas velocity perturbation is thought to represent a relatively frequently occuring condition. Although this point cannot be regarded as well established for the Cobra Dane location, it is estimated that perhaps 80 percent of all TIDs have amplitudes smaller than this value. TIDs of this scale (about 400 km wavelength) have little or no

7. Francis, S. H. (1973) Theory and Models of Atmospheric Acoustic-Gravity Waves and Travelling Ionospheric Disturbances, Bell Laboratories - Western Electric, Lincoln Laboratory (MIT), Joint Radar Propagation Study, pp 52, Whippany, N.J.

dependence on the level of geomagnetic activity. The numerical values selected for the simulated gravity wave were as follows:

Period	40 min
Phase Velocity	173 m/sec
Wavelength	415.2 km
Amplitude	50 m/sec
Phase	0° at 68°N and 160°E
Direction	180° true azimuth

A three-dimensional numerical ionosphere was generated from the ambient model perturbed by the TID with the following limits:

Latitude	49° to 85°	in 25 planes
Longitude	100° to 176°	in 20 planes
Altitude	90 km to 981 km	in 9 km intervals

This model is representative of the ionosphere North-West of the Cobra Dane location. Figure 5 is an example of the plasma frequency profile near the center of the grid. Subsequent ionospheres were generated in four-min intervals as the TID moved relative to the radar with the given velocity and direction.

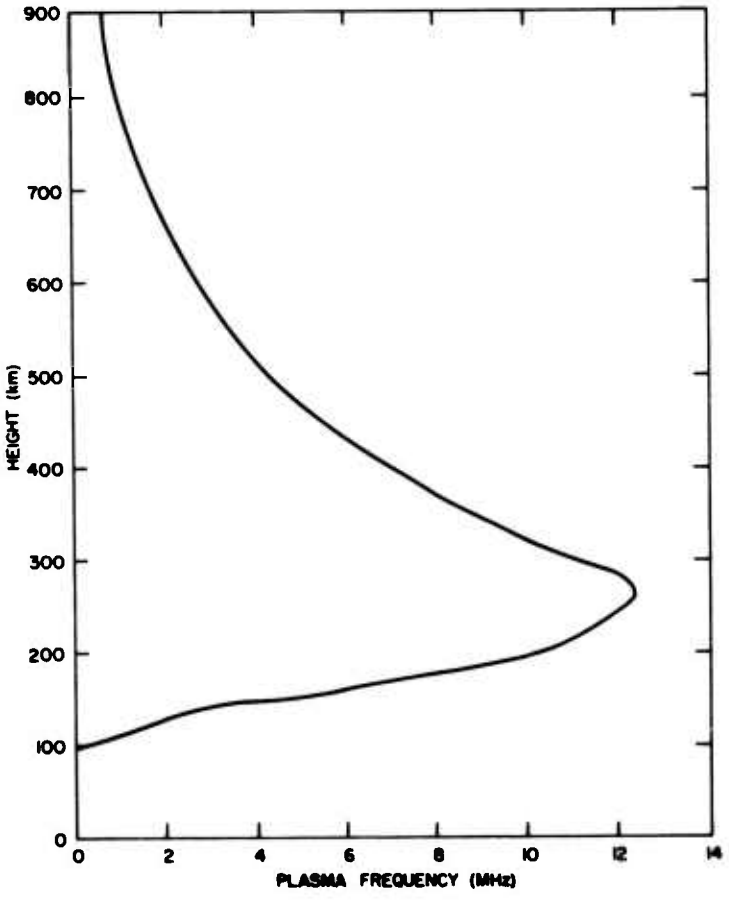

Figure 5. Model Ionosphere 160.6° Longitude, 30.0° Colatitude

5. RAY TRACING

Within the ionosphere a radar pulse travels more slowly than it does in free space and this causes the apparent range of the target to be greater than its true range. The range error or group delay can be calculated from a knowledge of how the refractive index varies along the propagation path by the use of ray-tracing techniques.

The three-dimensional ray-tracing computer program developed by Jones[8] and modified by Gibbs[9] was used in this study. The geographic coordinates of the ground transmitter used in the calculations were 37.55°N and 174.05°E, and the operating frequency selected was 1215 MHz. Rays were traced to a fixed point in space governed by the azimuth and elevation angle for that case. The terminal altitude for all cases was 900.000 km. The target coordinates for the various cases in degrees is shown in Table 1.

Table 1. Target Coordinates and True Range

Azimuth (°)	Elevation (°)	Colatitude (°)	Longitude (°)	True Range km
280	5	39.959892	135.089093	2992.5880
280	10	38.729107	140.845111	2568.2776
280	20	37.445249	149.990254	1947.2719
300	1	32.501181	125.243784	3994.6790
300	3	32.197038	128.699269	3186.5141
300	5	31.999184	131.969482	2992.5726
300	10	31.863319	139.247201	2568.2903
300	20	32.435392	150.070413	1947.2649
310	1	27.870227	124.137118	3994.6831
310	3	27.833096	128.149372	3186.4827
310	5	27.903034	131.886314	2992.5613
310	10	28.407578	139.980063	2568.2743
310	20	30.014323	151.377735	1947.2693
319	1	23.672611	124.333562	3994.6431
319	3	23.912131	128.940323	3186.5053
319	5	24.256924	133.141796	2992.5892
319	10	25.402452	141.904053	2568.2771
319	20	27.985155	153.445922	1947.2740
330	20	25.822861	157.256782	1947.2733
340	5	16.675713	144.790324	2992.5799
340	20	24.294104	161.972043	1947.2752
355	20	23.057399	170.839095	1947.2738

8. Jones, R. M. (1968) A three-dimensional ray-tracing computer program, Radio Sci. 3(1):93-94.

9. Gibbs, J. (1974) Private Communication.

Target location was specified to 0.000005 deg of latitude and longitude in order to locate the target to an accuracy of 0.5 m in radar range. The required change of the launching azimuth and elevation angle of the radar beam to hit the target area was in the order of several μ rad.

Figure 6 is a summary chart of the variation of group delay as a function of elevation angle. Although only data for an azimuth of 319° are shown, the values for the other azimuth angles were similar. To a first order approximation, the group delay is proportional to the TEC as illustrated in the same diagram.

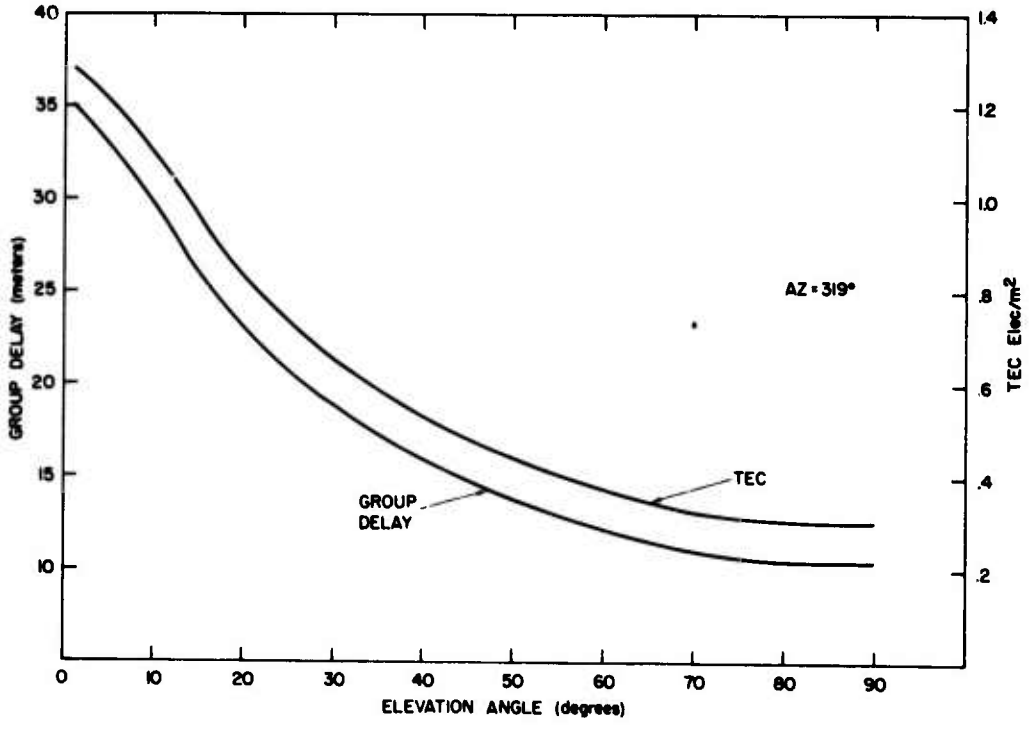

Figure 6. Variation of Group Delay as a Function of Elevation Angle

For each given azimuth and elevation angle, a ray path was calculated from the radar to the target for each four-min interval of the TID. Using zero times as a reference, the changes in the apparent range were computed and plotted as delay deviation against time in Figures 7 to 28. This delay deviation or variable component of group delay in the apparent range is the result of the time varying ionosphere. The 280° azimuth case simulates a radar propagation path nearly parallel to the TID phase fronts; while the 355° case is nearly parallel to the direction of travel of the TID, that is, almost perpendicular to the phase fronts.

The difference between the maximum and minimum of these curves represents the group delay. Thus, if a radar measurement is corrected by using the maximum value on this curve and the target is at the minimum value, the range error due to the TID would be the group delay. Table 2 and Figure 28 are a summary of the ray-tracing data. Although calculations were made from a TID heading due south, the data can be used to predict the group delay for other incoming TIDs since it is the relative angle between the radar propagation path and TID direction that is critical.

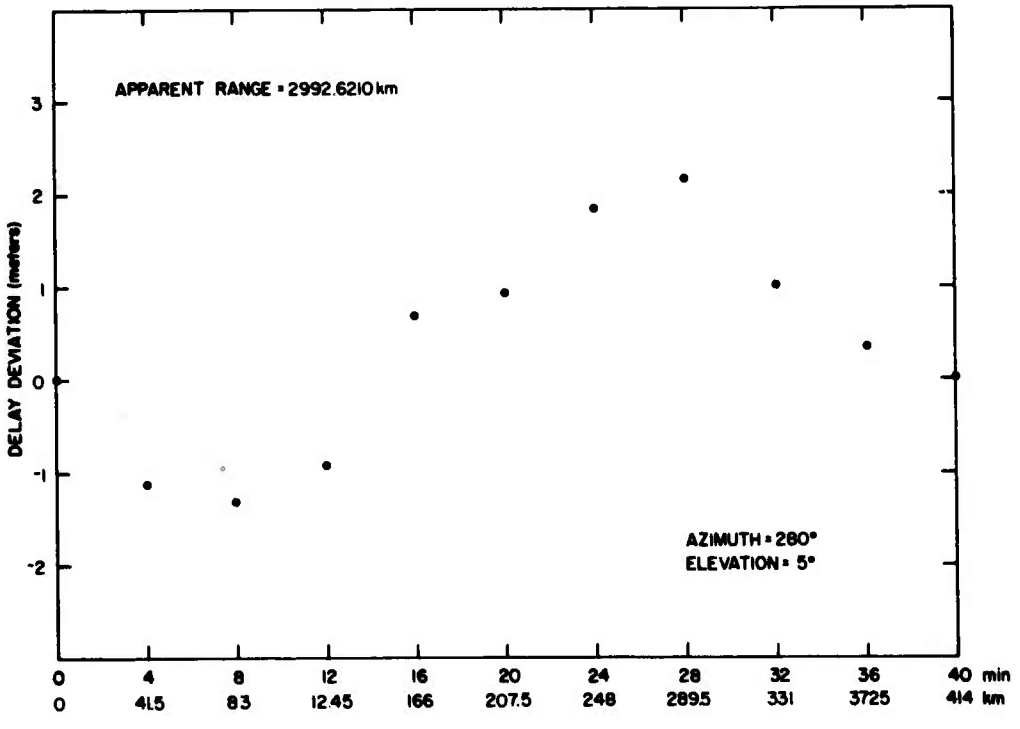

Figure 7. Change in Apparent Range as a Function of Time, Az = 280°, EL = 5°

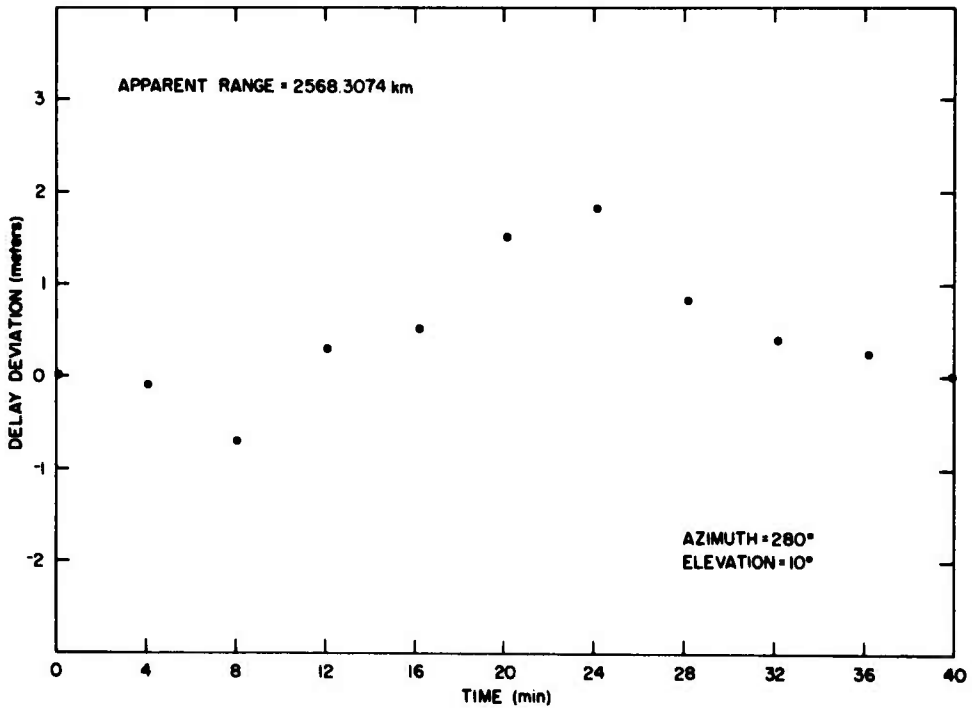

Figure 8. Change in Apparent Range as a Function of Time, Az = 280°, EL = 10°

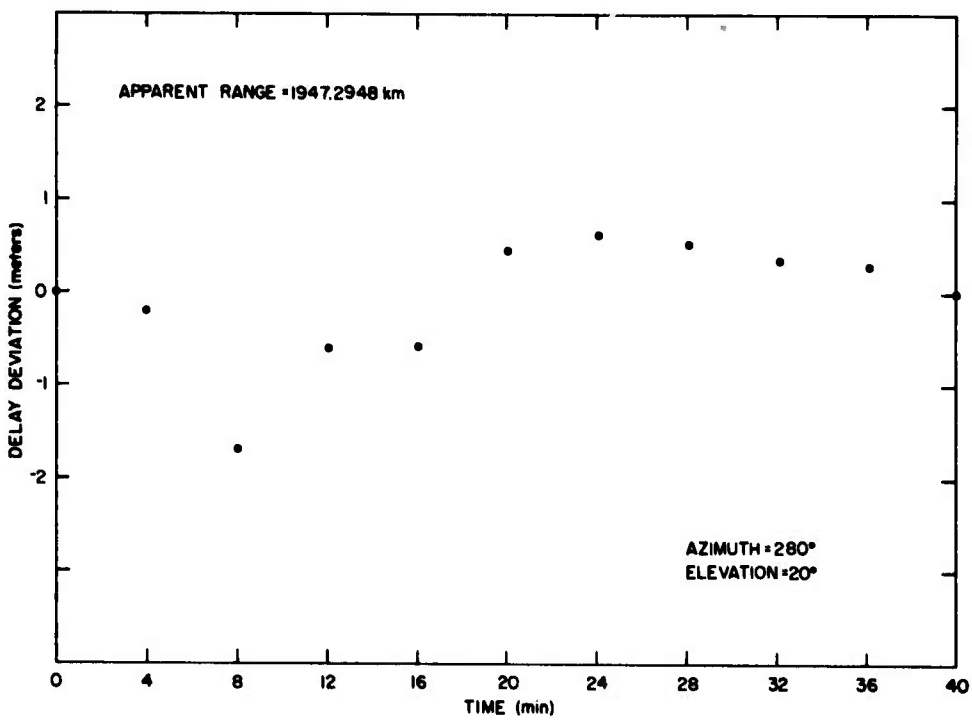

Figure 9. Change in Apparent Range as a Function of Time, Az = 280°, EL = 20°

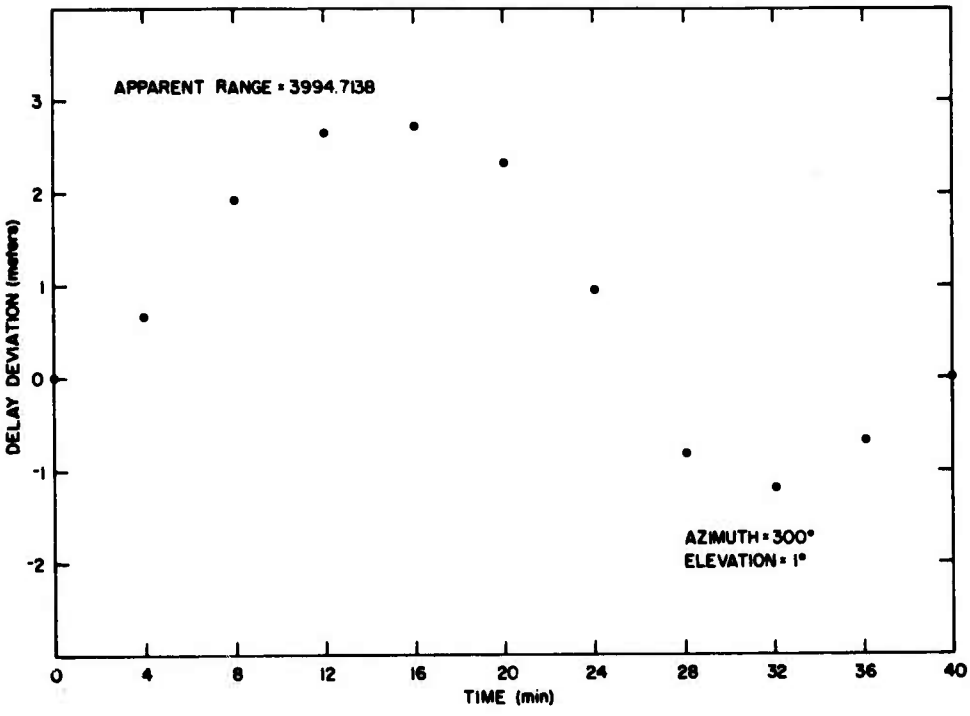

Figure 10. Change in Apparent Range as a Function of Time, Az = 300°, EL = 1°

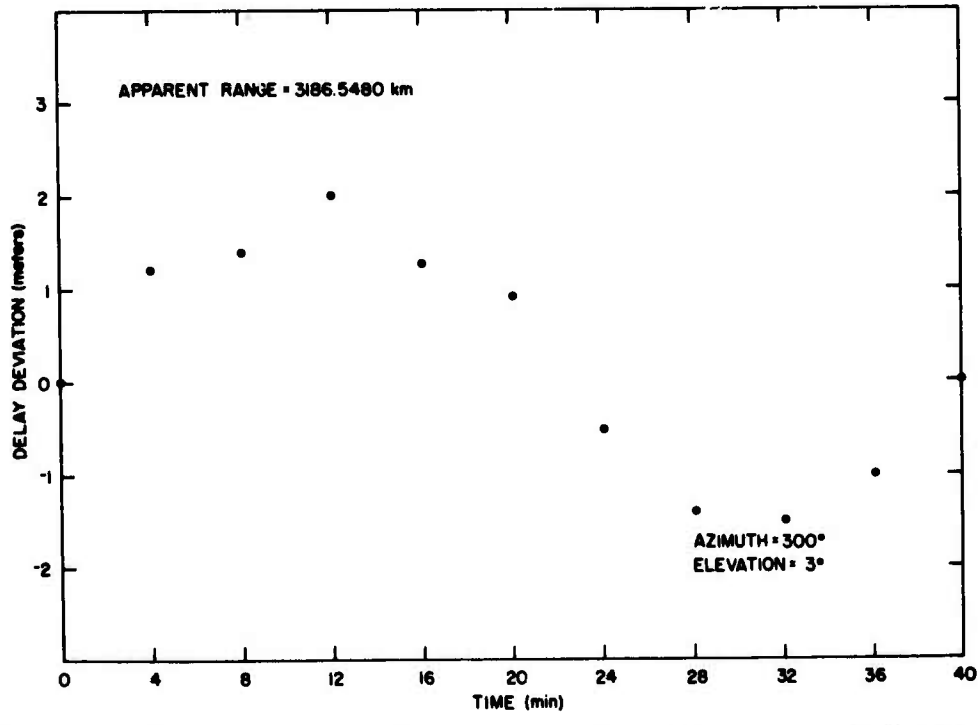

Figure 11. Change in Apparent Range as a Function of Time, Az = 300°, EL = 3°

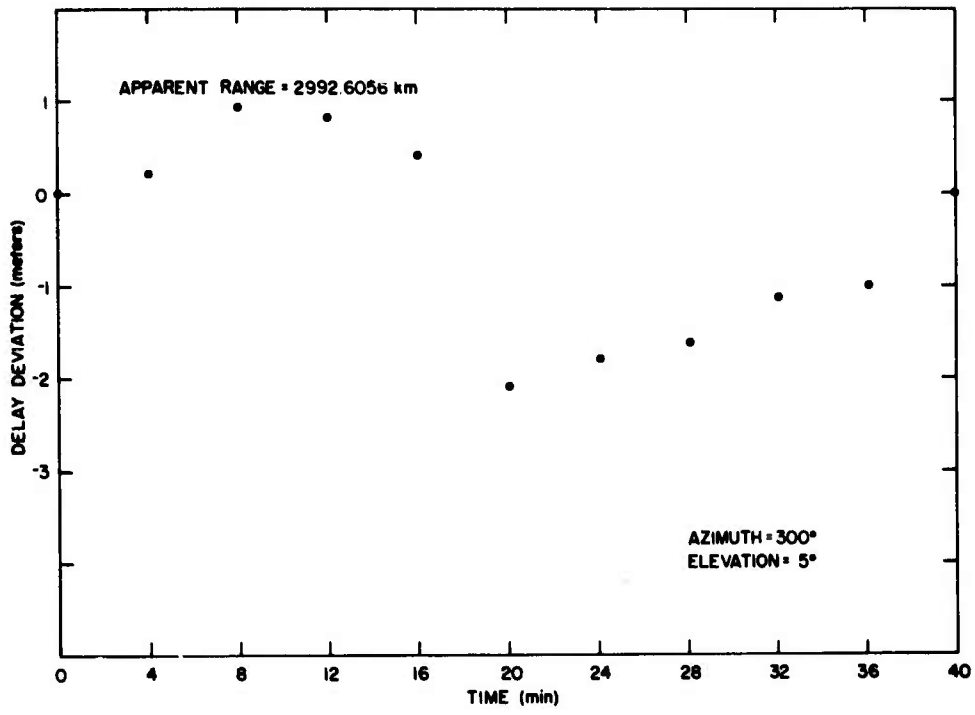

Figure 12. Change in Apparent Range as a Function of Time, Az = 300°, EL = 5°

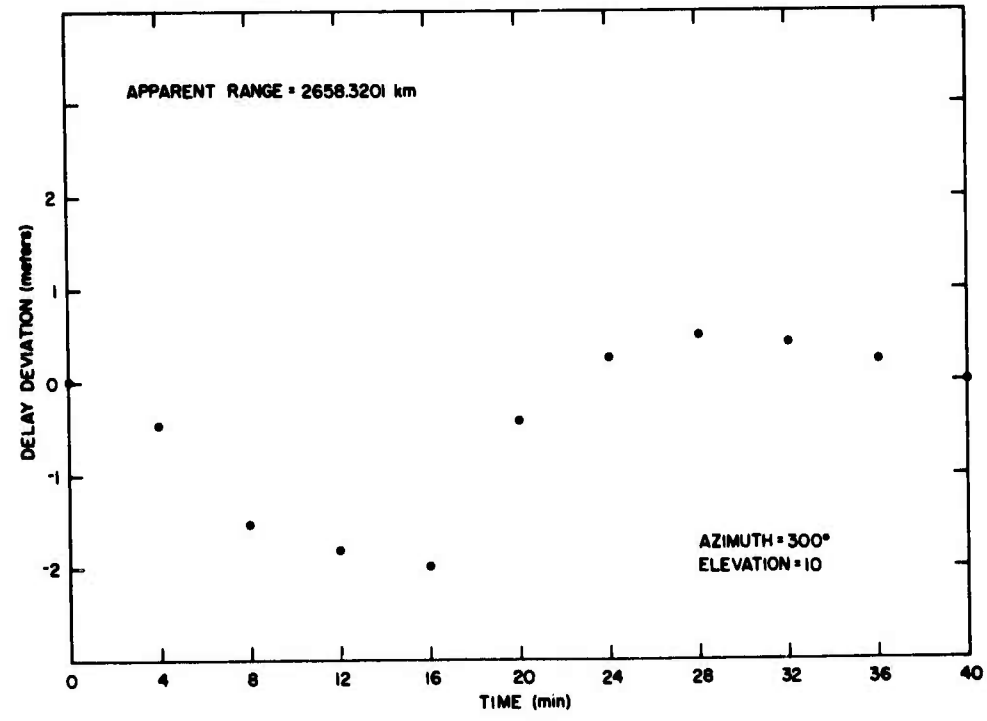

Figure 13. Change in Apparent Range as a Function of Time, Az = 300°, EL = 10°

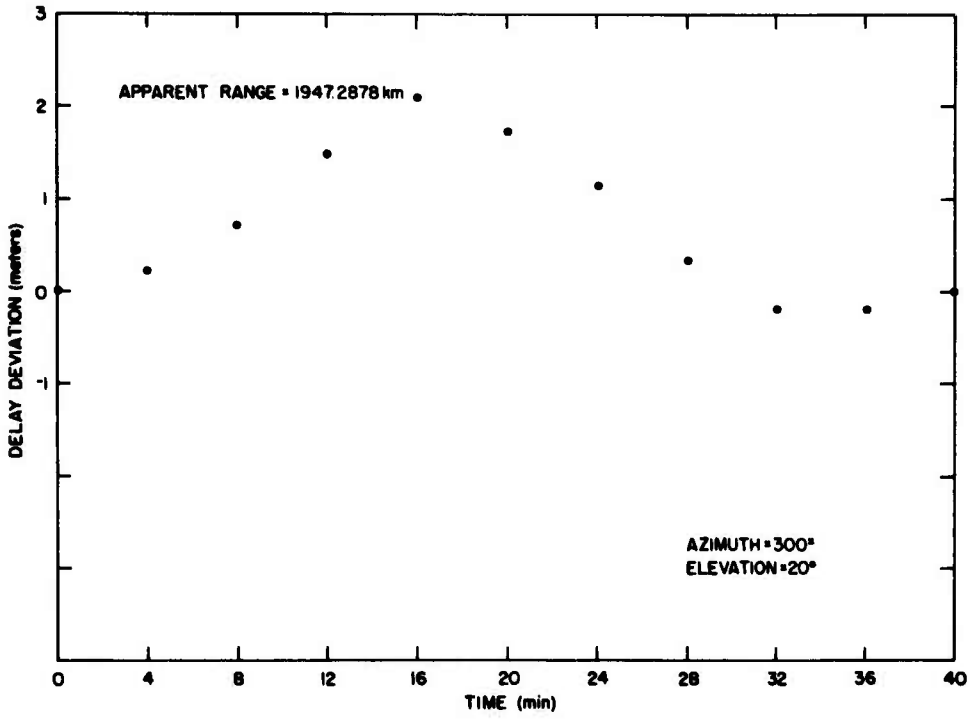

Figure 14. Change in Apparent Range as a Function of Time, Az = 300°, EL = 20°

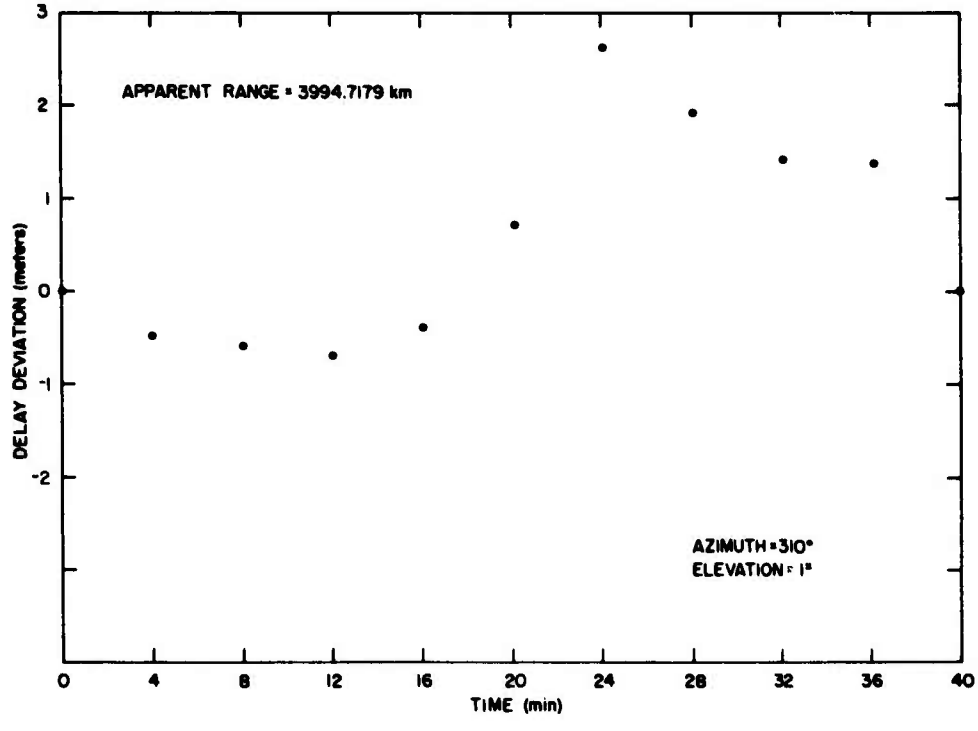

Figure 15. Change in Apparent Range as a Function of Time, Az = 310°, EL = 1°

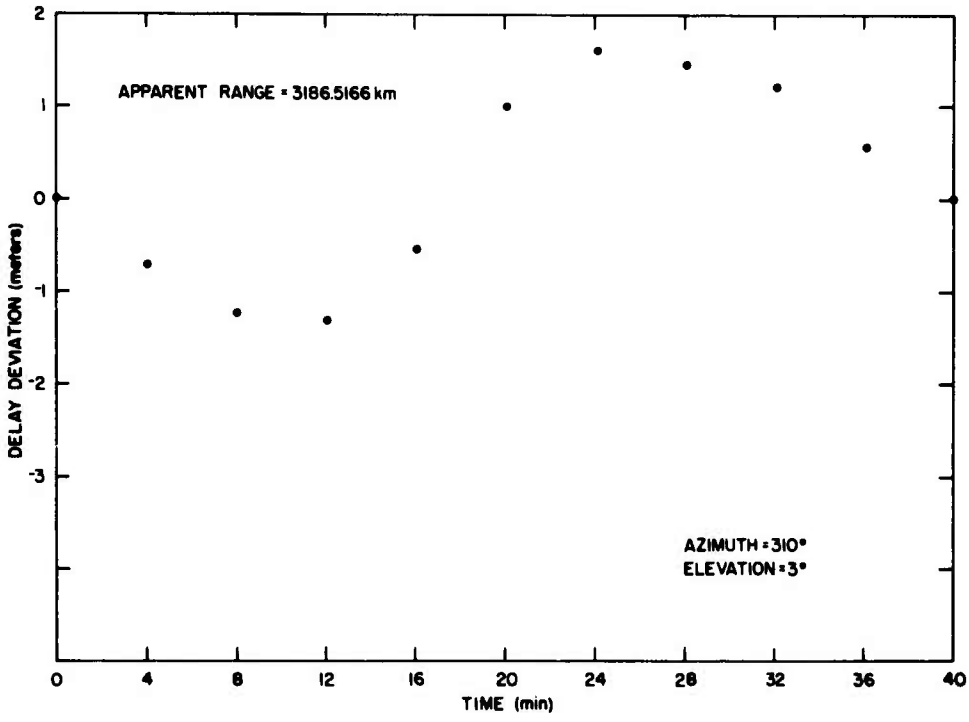

Figure 16. Change in Apparent Range as a Function of Time, Az = 310°, EL = 3°

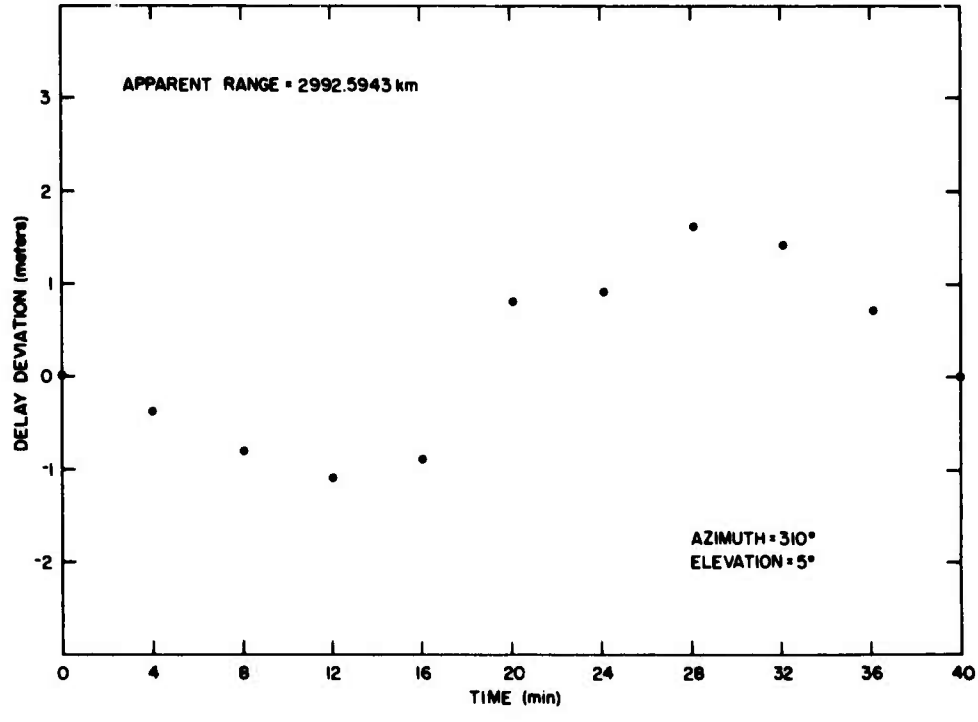

Figure 17. Change in Apparent Range as a Function of Time, Az = 310°, EL = 5°

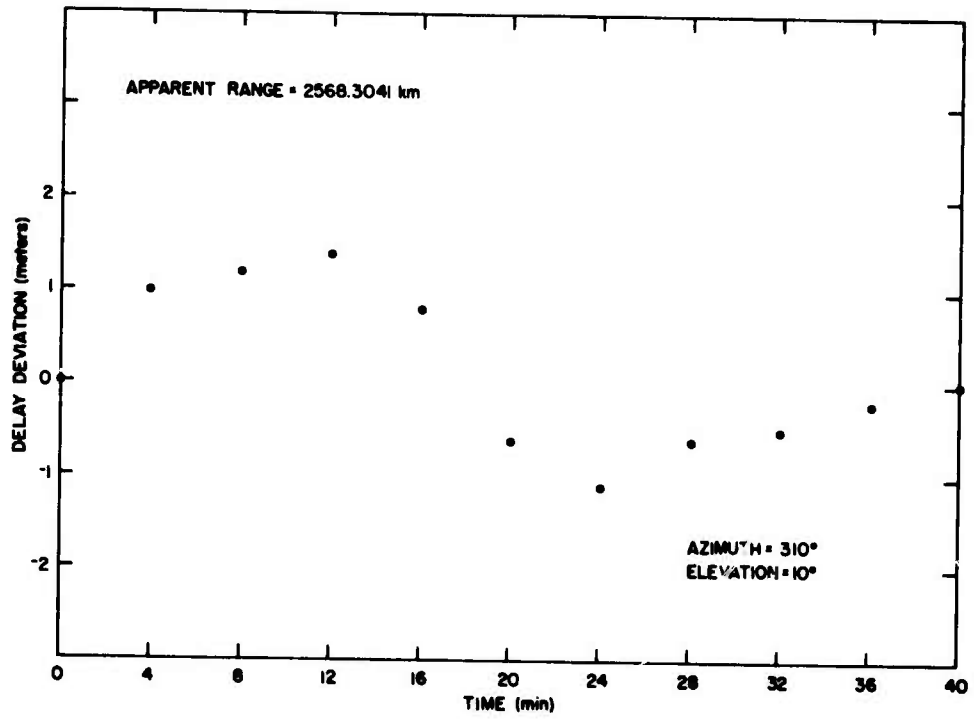

Figure 18. Change in Apparent Range as a Function of Time, Az = 310°, EL = 10°

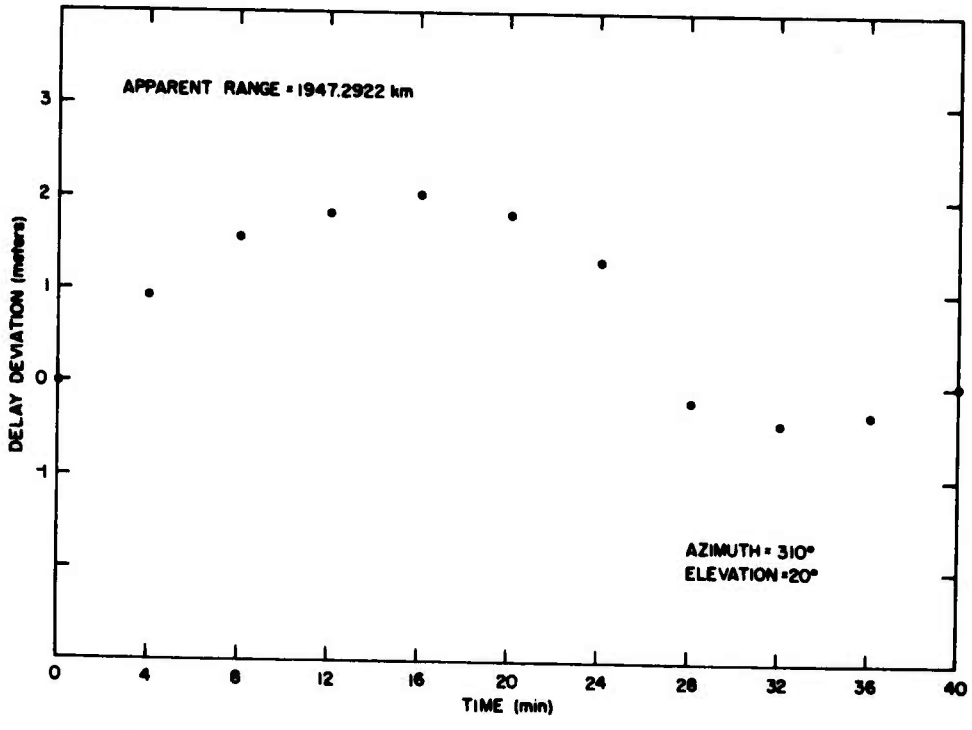

Figure 19. Change in Apparent Range as a Function of Time, Az = 310°, EL = 20°

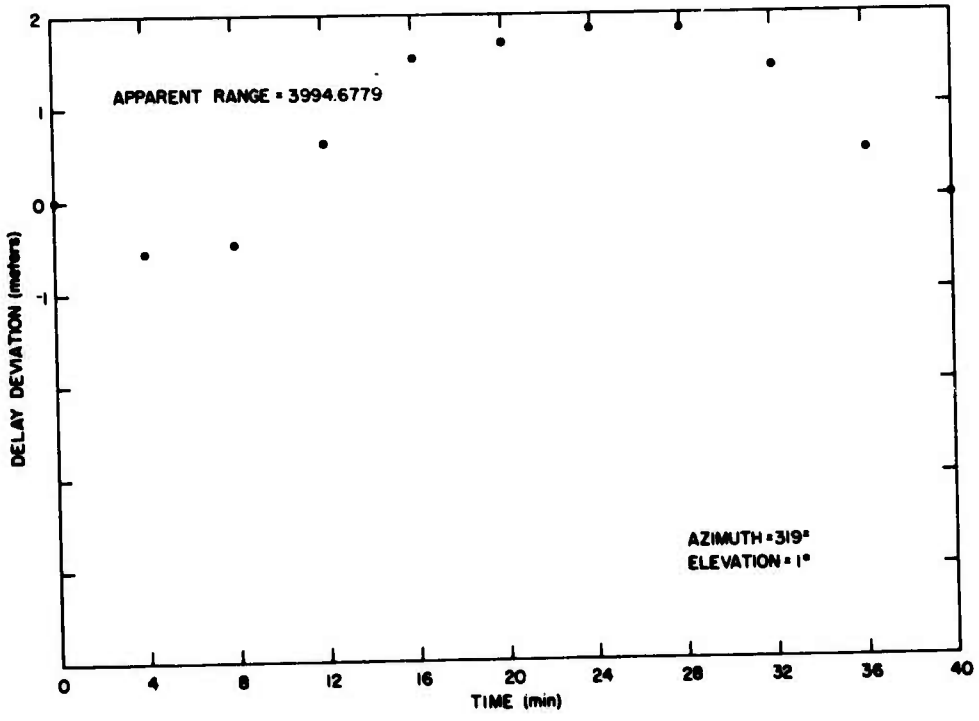

Figure 20. Change in Apparent Range as a Function of Time, Az = 319°, EL = 1°

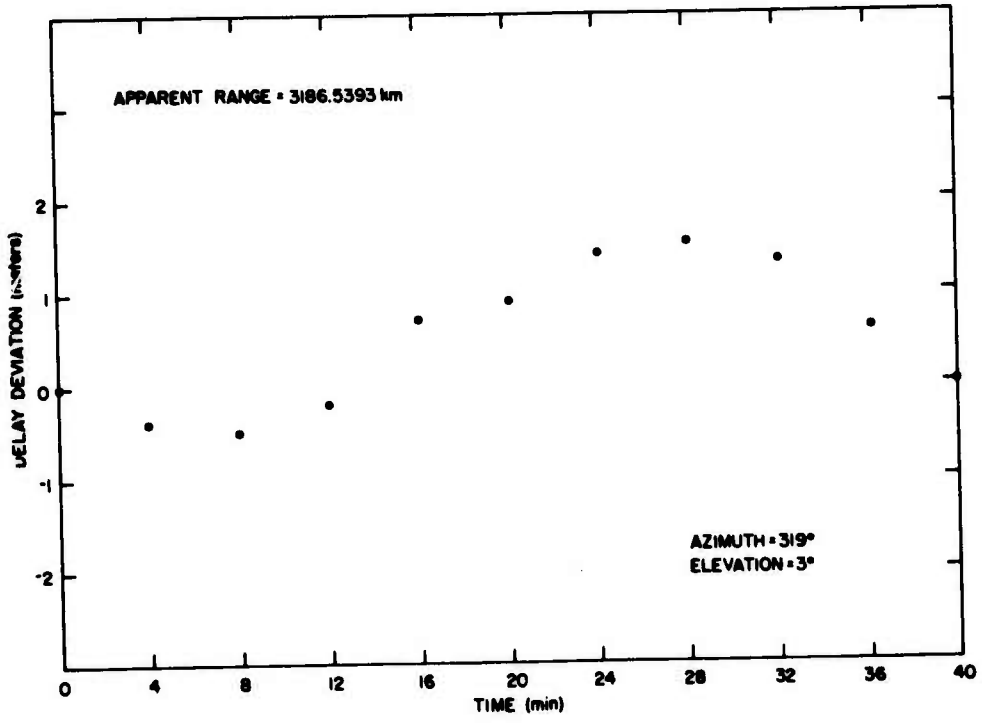

Figure 21. Change in Apparent Range as a Function of Time, Az = 319°, EL = 3°

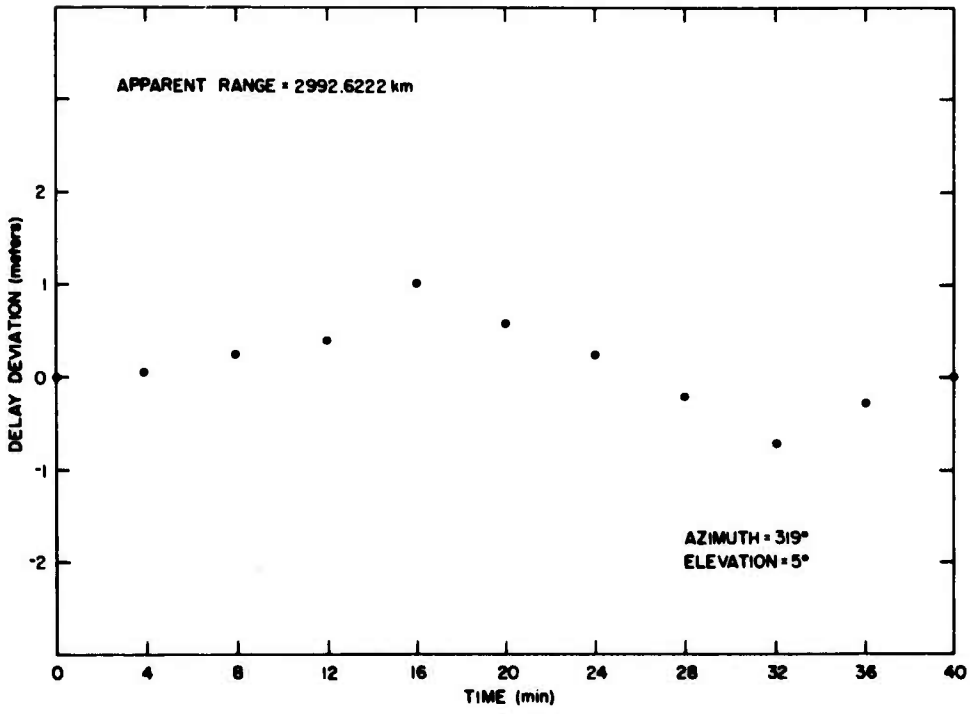

Figure 22. Change in Apparent Range as a Function of Time, Az = 319°, EL = 5°

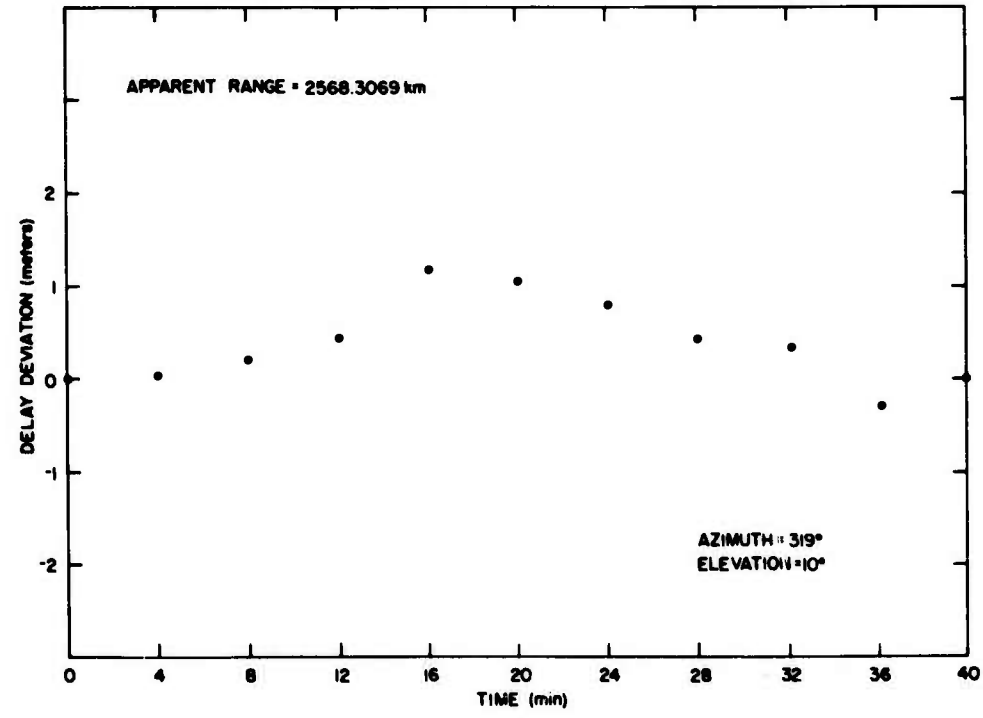

Figure 23. Change in Apparent Range as a Function of Time, Az = 319°, EL = 10°

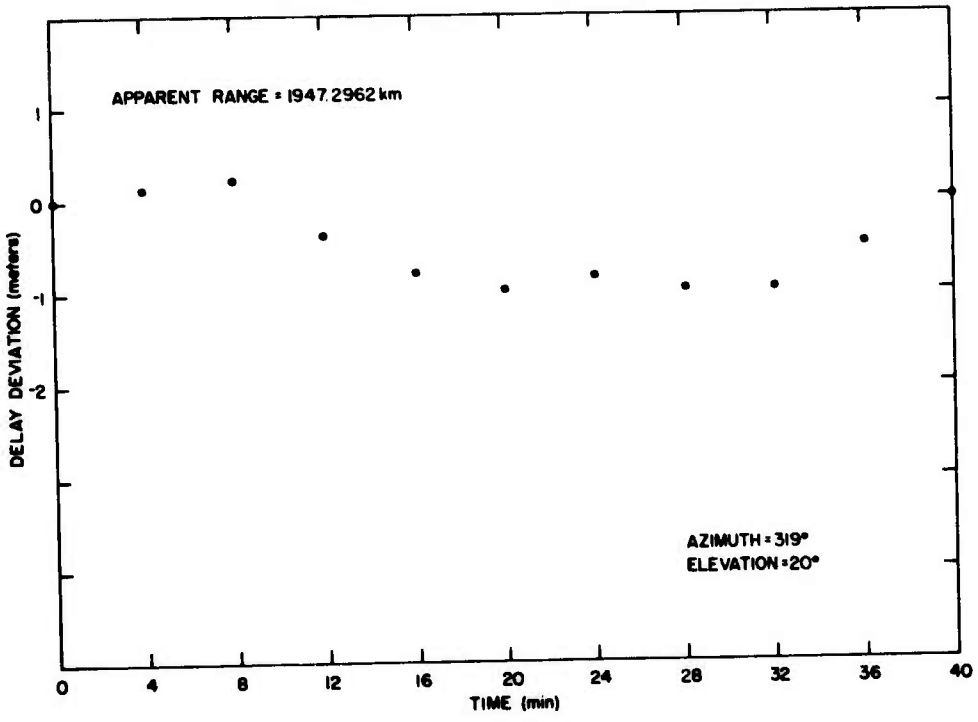

Figure 24. Change in Apparent Range as a Function of Time, Az = 319°, EL = 20°

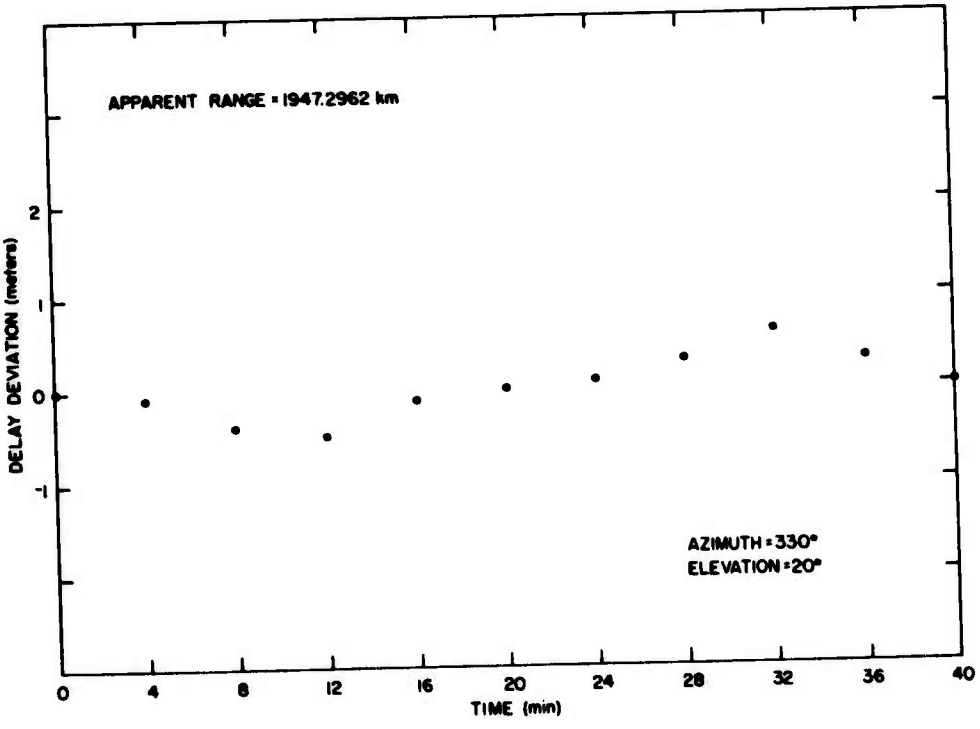

Figure 25. Change in Apparent Range as a Function of Time, Az = 330°, EL = 20°

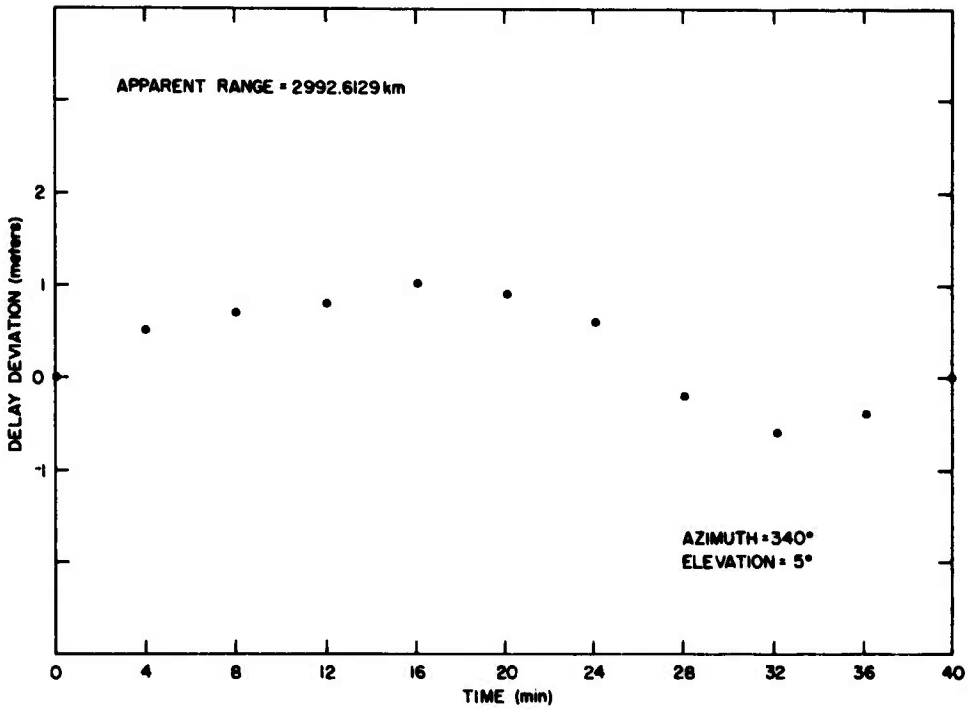

Figure 26. Change in Apparent Range as a Function of Time, Az = 340°, EL = 5°

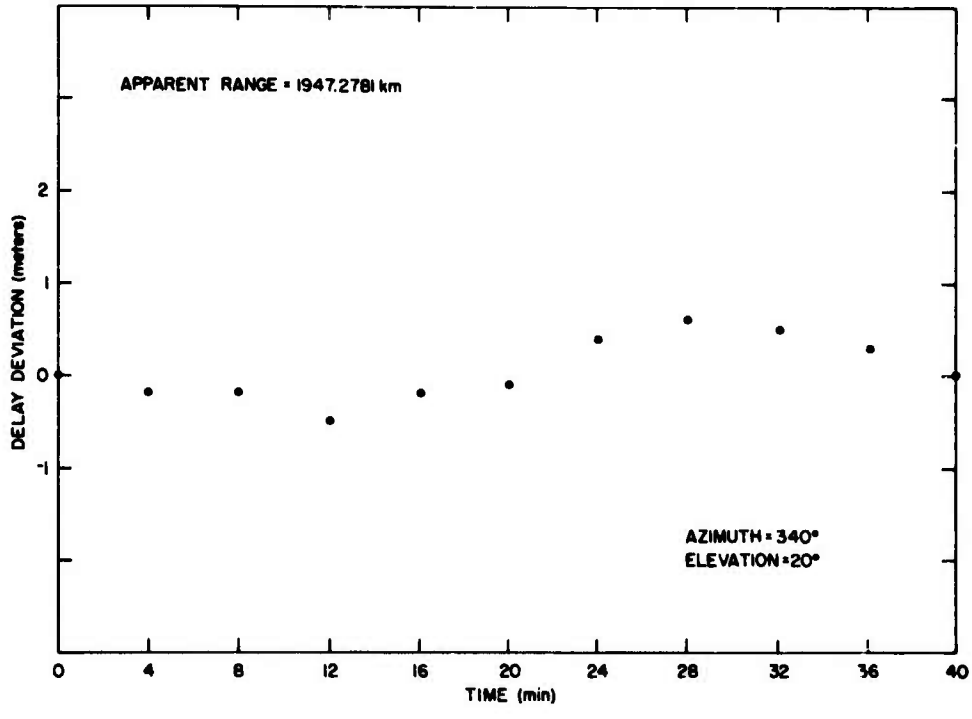

Figure 27. Change in Apparent Range as a Function of Time, Az = 340°, EL = 20°

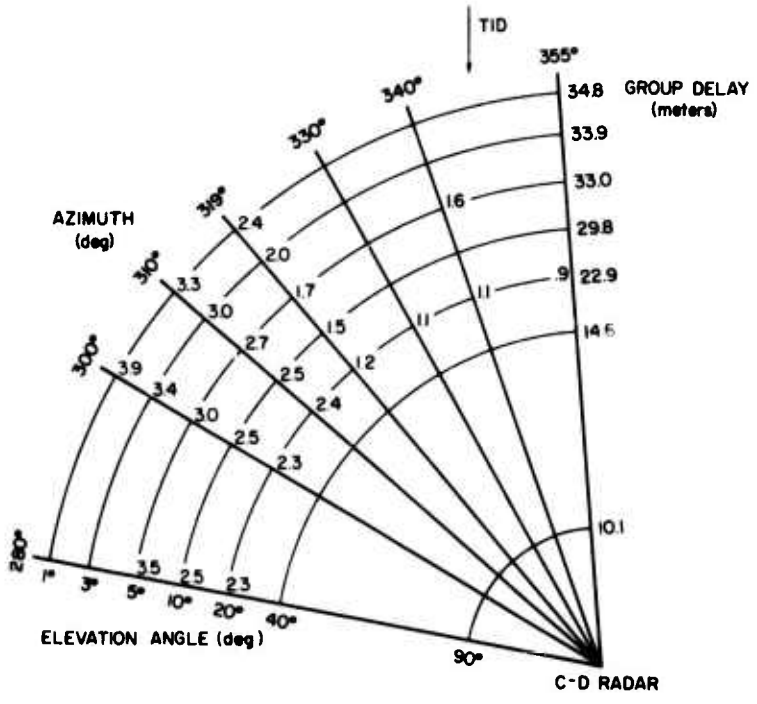

Figure 28. Variable Component of Group Delay in Meters

Table 2. Summary of Ray-Tracing Data

Elevation angle (°)	Group* delay m	Variable Group Delay** (m) function of Azimuth						
		280°	300°	310°	319°	330°	340°	355°
1	34.8		3.9	3.3	2.4			
3	33.9		3.4	3.0	2.0			
5	33.0	3.5	3.0	2.7	1.7		1.6	
10	29.8	2.5	2.5	2.3	1.5			
20	22.9	2.3	2.3	2.4	1.2	1.1	1.1	.9

*Group Delay = Apparent range-true range in meters = $\int(\mu - 1)ds$.

**Variable Group Delay = Variable component of ionospheric retardation as TID travels through medium expressed as (maximum apparent range-minimum apparent range) in meters.

The variable component of the group delay is dependent at a fixed frequency on the following quantities:

(a) The direction of TID travel relative to the propagation path, and

(b) the elevation angle.

When the direction of TID travel is within approximately ± 40° of the propagation path the variable component of the group delay will be less than 8 ft. For TID propagation outside these azimuth angles, the range error is greater than 8 ft for elevation angles less than 10°, for the particular case illustrated. It is possible to replot the above data so that the variable component of the group delay can be extrapolated for various elevation angles and directions of TID travel as illustrated in Figure 29. An eight-ft allowable error is shown for reference.

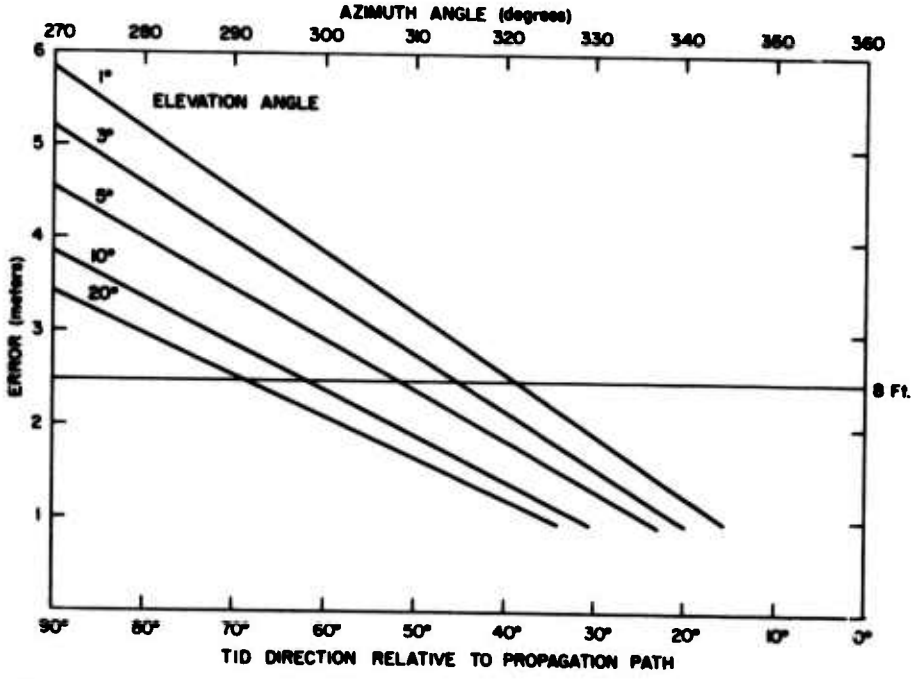

Figure 29. Extrapolated Range Error as a Function of TID Direction and Elevation Angle

6. CONCLUSIONS

A multifrequency ranging technique allows for real-time corrections for the excess propagation time delay introduced by the ionosphere in the overall transit

time between an L-Band Radar station and a high flying target. In a uniform ionosphere this correction can be applied over a large area. In a non-uniform ionosphere as caused by a TID, this correction is valid over a limited area. Ray-tracing techniques have been utilized to determine the effects of this irregular ionosphere for several special cases thought to represent a relatively frequently occurring condition. In particular, it was found that at 1215 MHz, the range errors were less than 2.5 m when the TID direction of travel was within ± 40° of the radar propagation path. Outside this azimuth angle, when the elevation angle was greater than 10°, the range error was less than 2.5 m.

Ionospheric data has been simulated using a realistic TID model together with an ambient Chapman electron density profile which covers the Cobra Dane search area and the range errors due to these irregularities calculated.

References

1. Munro, G. H. (1958) Travelling ionospheric disturbances in the F-region, Aust. J. Phys., 11(1):91-112.
2. Hines, C. O. (1960) Internal atmospheric gravity waves at ionospheric heights, Can. J. Phys., 38(11):1441-1481.
3. Hooke, W. H. (1968) Ionospheric irregularities produced by internal atmospheric gravity waves, J. Atmos. Terr. Phys., 30(5):795-824.
4. Georges, T. M. (1968) HF doppler studies of travelling ionospheric disturbances, J. Atmos. Terr. Phys., 39(5):735-746.
5. Francis, S. H. (1972) Propagation of internal acoustic gravity waves around a spherical earth, J. Geophys. Res., 77:4221.
6. Elkins, T. J. (1972) High resolution measurements of ionospheric refraction, Space Research XII, pp. 1215-1220, Akademie-Verlag, Berlin.
7. Francis, S. H. (1973) Theory and Models of Atmospheric Acoustic-Gravity Waves and Travelling Ionospheric Disturbances, Bell Laboratories - Western Electric, Lincoln Laboratory (MIT), Joint Radar Propagation Study, pp 52, Whippany, N. J.
8. Jones, R. M. (1968) A three-dimensional ray-tracing computer program, Radio Sci. 3(1):93-94.
9. Gibbs, J. (1974) Private Communication.